

# Multi-stage stochastic framework for energy management of virtual power plants considering electric vehicles and demand response programs



F. Sheidaei, A. Ahmarinejad\*

Department of Electrical Engineering, Yadegar-e-Imam Khomeini (RAH) Shahre Rey Branch, Islamic Azad University, Tehran, Iran

## ARTICLE INFO

### Keywords:

Virtual power plant  
Islanded microgrid  
Multi-stage stochastic programming  
Electric vehicles  
Demand response  
Renewable energy resources

## ABSTRACT

Nowadays, the importance of the coordinated operation of power system assets has caused severe challenges that can be addressed through some recently emerged concepts, such as microgrids (MGs) and virtual power plants (VPPs). In this paper, a hierarchical model is proposed for simultaneous modeling of an MG scheduling and VPP energy management problems. Given the stochastic nature of the scheduling inputs, power production and also, load demand uncertainties are modeled using a scenario-based method. Therefore, the final model is presented as a stochastic mixed-integer linear programming (MILP) model. It is possible to cover the fluctuations at the minimum cost using demand response (DR) programs and electric vehicles (EVs). In addition, the possibility of power transaction between the adjacent MGs is analyzed in scheduling model, preventing unreal power exchanges. The simulation results indicate that the coordinated operation of MGs can improve load restoration, and reduce the load supply costs in each MG. It is also observed that the profit of the VPP would be higher in the case with the time-of-use (TOU) tariff compared to the cases with the real-time pricing (RTP) and critical peak pricing (CPP) mechanisms.

## 1. Introduction

### 1.1 Motivation

The microgrid (MG) concept reflects the integration of distributed energy resources (DER), which can be operated in two modes, namely grid-connected and islanded modes. In general, MGs play an important role in the transformation of the existing power grids into smart grids. MGs are often used in the grid-connected mode to minimize the costs. They are also used in the islanded mode to increase reliability. The connection of MGs results in the formation of a hybrid network, which helps reduce the network operating costs in the grid-connected mode, and mitigate load curtailments in the islanded mode compared to individual MGs. Furthermore, the virtual power plant (VPP) concept refers to an integrated set of loads, DERs, and energy storage systems (ESSs). A VPP is operated in two modes, either as a technical VPP (TVPP) or commercial VPP (CVPP). The system owner should take into consideration the constraints relating to the operation of DERs, VPPs' loads, system voltage and frequency levels, and the system conditions (in the context of TVPP). The system owner should try to improve system reliability and reduce the system operating cost (in the context of CVPP) based on the aforesaid constraints. The owner of a VPP schedules its loads and DERs with respect to the market price. When the

market price is high, the VPP owner curtails a part of the load and maximizes the generation by the DER. Consequently, the VPP supplies its load locally, and purchases a small portion of its energy from the market (systems other than the VPP). In addition, when the market price decreases, the owner of the VPP reduces the generation of its DERs, puts its entire load into the system, and purchases a large portion of the energy from the market [1].

In this paper, a hierarchical method is proposed for the energy management of MGs and VPPs. In this analysis, the optimal scheduling and a feasibility analysis of the coordinated scheduling of MGs are carried out based on the resilience index. The objective functions of the proposed framework for the MG and VPP are respectively operating cost minimization, and profit maximization due to the power exchange with the upstream network.

### 1.2 Literature review

Today, the ever-increasing penetration of renewable energy sources (RES) has led to new challenges to MG energy management. The common methods used in the studies for uncertainty management include robust optimization [2], and stochastic optimization [3] techniques. In [2], a robust optimization technique is utilized for the optimal scheduling of MGs with electrical storage systems (ESSs) and direct load

\* Corresponding author.

E-mail address: [ahmarinejad@gmail.com](mailto:ahmarinejad@gmail.com) (A. Ahmarinejad).

control (DLC). The results of this study reveal the effective role of DR programs in determining the efficiency of renewable resources. The authors of [3] proposed a multi-time model involving multiple energy carriers for the optimal MG scheduling. In the day-ahead scheduling model, the uncertainty of RES is modeled under different scenarios, and the energy management system seeks to minimize the total operating cost. However, in the scheduling model with a 5-min resolution, the fluctuations of the RES are alleviated using controllable loads and energy transaction.

The studies on the method of modeling MGs and their relation with each other can be classified into two main categories: (a) individual modeling of an MG, (b) modeling several interconnected MGs. In [4], a centralized energy management system is introduced for MG energy management in the islanded mode. This system uses the predictive control technique to properly operate the ESSs. In [5], a decentralized energy management system is developed for the coordinated operation of MGs in a distribution system. The goal is to minimize the operating costs in the grid-connected mode and ensure power stability in the islanded mode. In [6], a hybrid energy management system is proposed as a hierarchical system for the optimization of the power transaction, energy storage, and distribution of energy in smart grids comprised of individual or interconnected MGs. The advantages and disadvantages of three energy management systems are thoroughly explained and compared in [7]. In [8], a new method has been suggested to coordinate the installation of storage systems, mainly to prevent the cascaded and consequent failure of generating units in MGs. In this method, if the voltage in the DER terminals is not improved following an error within the period specified in the network, scheduling is carried out to install a storage system at the high-potential buses. In [9], a new energy management system is designed for an MG, consisting of an incentive-based demand response program (DRP) and different market mechanisms. A two-layer energy management system is developed in [10] to improve the users' condition at the end points of the feeder in MGs with ESSs due to the high cost of storage systems. In [11], a two-layer hierarchical control scheme is proposed for the compensation of voltage unbalance so that the voltage variations of all buses will remain in the permitted range after changing the operation mode. In [12], a robust energy management system is introduced using the information-gap decision theory (IGDT) for MGs, operating in the islanded mode. This system takes into account the system frequency stability simultaneously. In [13], a battery energy management system (BEMS) is proposed for MGs with solar panels. This system reduces the generation cost and controls the charging and discharging decisions to increase the battery lifetime concurrently. A stochastic scheduling optimization model is presented in [14] to minimize the MG operating cost under severe uncertainty within a risk-constrained framework.

In [15], a new control method is proposed for the energy management of multiple MGs in a distribution system where each MG and the distribution network operator (DNO) are considered individual entities with their own goals. Ref. [16] discussed the role of grid-connected MGs as smart grids in increasing the power system flexibility against extreme events. A new hybrid two-level energy management system is introduced in [17] by considering the point of common coupling (PCC) constraint. It is stated in [18] that coordinated and integrated MG scheduling is useful and cost-effective for MG owners and consumers. In this study, two pricing models based on the time-of-use (TOU) and real-time pricing (RTP) are employed to model the DR program. In [19], a two-stage energy management strategy is developed for grid-connected MGs considering high renewable energy penetration.

In the case of VPPs, it is possible to carry out the scheduling for different sectors and model various objective functions, including the cost and benefit functions. Moreover, it is possible to combine the energy market and the deregulated power system concepts. As can be observed in the literature, the concept of VPP in the energy market or ancillary service market can be modeled, taking into consideration different time resolutions. In [20], a model is proposed to find

equilibrium for a VPP. In the proposed model, the behavior of every generator is modeled using a bi-level mathematical program with equilibrium constraints (MPEC). In [21], a bi-level scheduling model is developed for VPPs with considerable controllable load and numerous RESs. In [22], a new binary backtracking search algorithm (BBSA) is proposed to control DERs in MGs. In [23], a uniform market clearing model is developed based on the centralized energy management system of VPPs to improve the competition between the DERs. In the proposed method, a scenario-based model is used to model the unpredictable system behavior. In [24], a VPP with conventional and RESs is modeled for participating in the wholesale market. The overarching goal of this study was to introduce a framework for maximizing the VPP profit through day-ahead and 5-min scheduling. To this end, the VPP purchases energy from a wholesale market and then, locally sells it to consumers in its territory. In [25], a decision-making tool is developed to maximize the profit of VPPs in the energy and ancillary service markets. In this research, a dynamic flexible formulation is proposed, which is applicable to different market mechanisms. Besides, the scheduling problem is solved over a mid-term horizon, e.g. from one week to one year and a short-term horizon, i.e. one hour to 168 h. In [26], a structure, including both heat and electricity is introduced in the form of a multi-energy VPP (MVPP). The MVPP is allowed to participate in the energy market and optimally support its heating system, considering the energy market price.

Ref. [27] proposed an energy management system for a VPP, which includes solar PV panels, wind turbines, ESSs, combined heat and power (CHP) units. The main objective beyond implementing the mentioned day-ahead scheduling model is to maximize the profit and minimize the emissions, while characterizing uncertainties of the problem using a scenario-based optimization technique. A multi-objective optimization model has been developed in [28], taking into account the operation cost, risk, and emission for scheduling DERs, consisting of wind and solar energy systems, a biofuel generation unit, micro-turbines, an ESS, besides flexible loads. Ref. [29] describes the demerits associated with using individual uncertainty characterization methods and proposes a combined interval and deterministic optimization framework to tackle the optimal operation of a VPP. Ref. [30] has carried out a comprehensive review on the objective functions and constraints of the VPP scheduling problem, emphasizing on the uncertainties caused by load demand, renewable power generation, and market price. Ref. [31] proposes an overarching review on the MG and VPP scheduling problems by categorizing the objective functions, constraints, as well as uncertainty sources. Ref. [32] developed a model for scheduling a VPP in the presence of uncertainties due to wind power generation and price in a network with industrial assets. Moreover, a risk management strategy has been utilized to study probabilistic failures.

Ref [1] proposed a model for VPP scheduling aimed at maximizing the profit, i.e. minimizing the operating cost and maximizing the revenue. In addition, the mentioned reference has used CPP, TOU, and RTP mechanisms for the power transaction with the main grid. It is noteworthy that the current manuscript proposed a three-stage stochastic optimization framework for maximizing the VPP profit, taking into consideration different pricing mechanisms, network configuration, and power flow in the IEEE 118-bus distribution system. Furthermore, the VPP scheduling is carried out with respect to the optimal scheduling of each microgrid.

### 1.3 Contribution

The above-mentioned references studied MG energy management and VPP scheduling problems individually. In this regard, this paper presents a three-stage model to study the relationship between the MG and VPP so that the VPP maximizes its profit with respect to the optimal scheduling of the MG. Since the MG scheduling problem aims at minimizing the total operating cost, the final solution must meet the

total cost minimization and VPP profit maximization. Furthermore, the network configuration and power flow equations have been applied to the model to avoid any unreal power transaction, while considering the uncertainties caused by load demand forecast error and intermittent renewable power generation.

The main contributions of this paper are as follows:

- (i) Proposing a three-stage stochastic mixed-integer linear programming (MILP) framework for simultaneous energy management of MGs and the VPP in the presence of electric vehicles (EVs) and DRPs.
- (ii) Determining the service area of each MG, taking into consideration the network configuration.
- (iii) Studying the coordinated and uncoordinated operation of MGs to avoid any unreal power transaction.
- (iv) Maximizing the VPP profit with respect to the optimal scheduling of each MG.
- (v) Investigating the impact of pricing mechanisms, i.e. time-of-use (TOU), real-time pricing (RTP), and critical peak pricing (CPP) on the VPP profit.

### 1.4 Paper organization

The rest of this paper is arranged as follows:

Section 2 includes the developed energy management model. The mathematical formulation of the problem is proposed in Section 3. The presented algorithm is detailed in Section 4. Section 5 represents the simulation results, and lastly, some relevant conclusions are drawn in Section 6.

## 2. Energy management model

The first stage of the proposed method includes the linear programming model for the optimal formation of dynamic MGs, their service areas, and the optimal management of different technologies, such as ESSs, demand-side management programs and distributed generation (DGs) units. The second stage is about solving the optimal power flow problem in each service area for all dynamic MGs. Optimal power flow is carried out in the connected mode for each dynamic MG and the amount of power transaction is calculated. In the third stage, the MG scheduling is carried out within the service area of the VPP based on the energy price variations and the solution obtained from the previous stages. The main goal of stage three is to reduce the unbalance costs in real conditions using the DRPs and EVs, and to increase the energy sale profit utilizing different market pricing models. The overview of different stages of the presented model is indicated in Fig. 1.

## 3. Problem formulation

### 3.1. Determining the MG service area

The objective function relating to determining the service area of each MG is stated as maximization of the load restoration error in each MG as (1).

$$\max: F1 = \sum_{i \in T} \sum_{i \in N} (Pr_{i,t}^L \times \sum_{k \in K} P_{i,k,t}^{L,s}) \quad (1)$$

In the objective function above designed to determine the MG service area in the network,  $Pr_{i,t}^L$  denotes the load priority and  $P_{i,k,t}^{L,s}$  represents the load that can be supplied in every MG in the islanded mode. In this stage, with respect to the generating units that are categorized into primary and secondary groups depending on their capacity, the maximum power of each unit is specified and assets of each MG are determined. The above-mentioned objective function is subjected to the following constraints:

- **Connection constraint:** Due to the technical limitations, each bus can be allocated to one MG or even no MGs.

$$\sum_{k=1}^{N_{MGs}} \alpha_{i,k} \leq 1 \quad (2)$$

- **Slack bus condition:** Bus  $i$  may belong to the  $k$ th MG if and only if the slack bus belongs to the  $k$ th MG. The slack bus is the one with the main generating unit.

$$\alpha_{i,k} \leq \alpha_{r,k} \quad (3)$$

- **The parent bus condition:** To connect the  $i$ th bus to an MG, at least one of its parent buses has to belong to that MG. The parent bus is the first bus in the path between bus  $i$  and the slack bus corresponding to the MG.

$$\alpha_{i,k} \leq \sum_{\forall j \in \xi_{i,k}} \alpha_{j,k} \quad (4)$$

- **The radial condition:** In order to guarantee the radial structure of the MGs, an active power transmission path should exist between each bus and the slack bus corresponding to the MG. Therefore, in order to operate one feeder, the buses at the two ends should belong to the same MG; otherwise, that feeder cannot be operated.

$$\begin{aligned} B_l &\leq \alpha_{i,k} \\ B_l &\leq \alpha_{j,k} \\ B_l &\geq \alpha_{i,k} + \alpha_{j,k} - 1 \end{aligned} \quad (5)$$

### 3.2. Energy management in MGs

The objective function of the second stage can be mathematically stated as follows [33]:

$$\begin{aligned} \min: F2 & \\ &= \sum_{t=1}^T (C_{i,t}^{CG} + SUC_{i,t}^{CG} \times x_{i,t}^{SU} + SDC_{i,t}^{CG} \times x_{i,t}^{SD} + C_{i,t}^{ES} + C_{i,t}^{CL} + C_{i,t}^M) \end{aligned} \quad (6)$$

The objective function includes six parts as power supply cost, start-up and shut-down costs of the local power plants, the cost of using the storage equipment, the cost of using controllable loads, and the cost of transacting energy with the upstream network. In the scheduling process, the MGs with the same operation service areas are scheduled with an integrated approach, whereas the MGs incapable of transacting power with other MGs are scheduled individually. The minimization of the objective function (6) is subjected to the following constraints:

- **Thermal generating units:** The operation of thermal generating units that are within the service area of each MG involves operation constraints, such as the minimum and maximum power generation, the ramping rates, and decision variables relating to the status of units. These constraints are expressed through equations (7–12).

$$C_r^{CG} = \chi_t^{CG} a^{CG} + b^{CG} P_t^{CG} \quad (7)$$

$$P^{CG} \chi_t^{CG} \leq P_r^{CG} \leq \bar{P}^{CG} \chi_t^{CG} \quad (8)$$

$$P_t^{CG} - P_{t-1}^{CG} \leq Ramp_{CG}^{Up} \quad (9)$$

$$P_{t-1}^{CG} - P_t^{CG} \leq Ramp_{CG}^{Down} \quad (10)$$

$$\chi_t^{CG} - \chi_{t-1}^{CG} \leq \chi_t^{SU} - \chi_t^{SD} \quad (11)$$

$$\chi_t^{SU} + \chi_t^{SD} \leq 1 \quad (12)$$

- **Storage systems:** To operate storage systems, the constraints

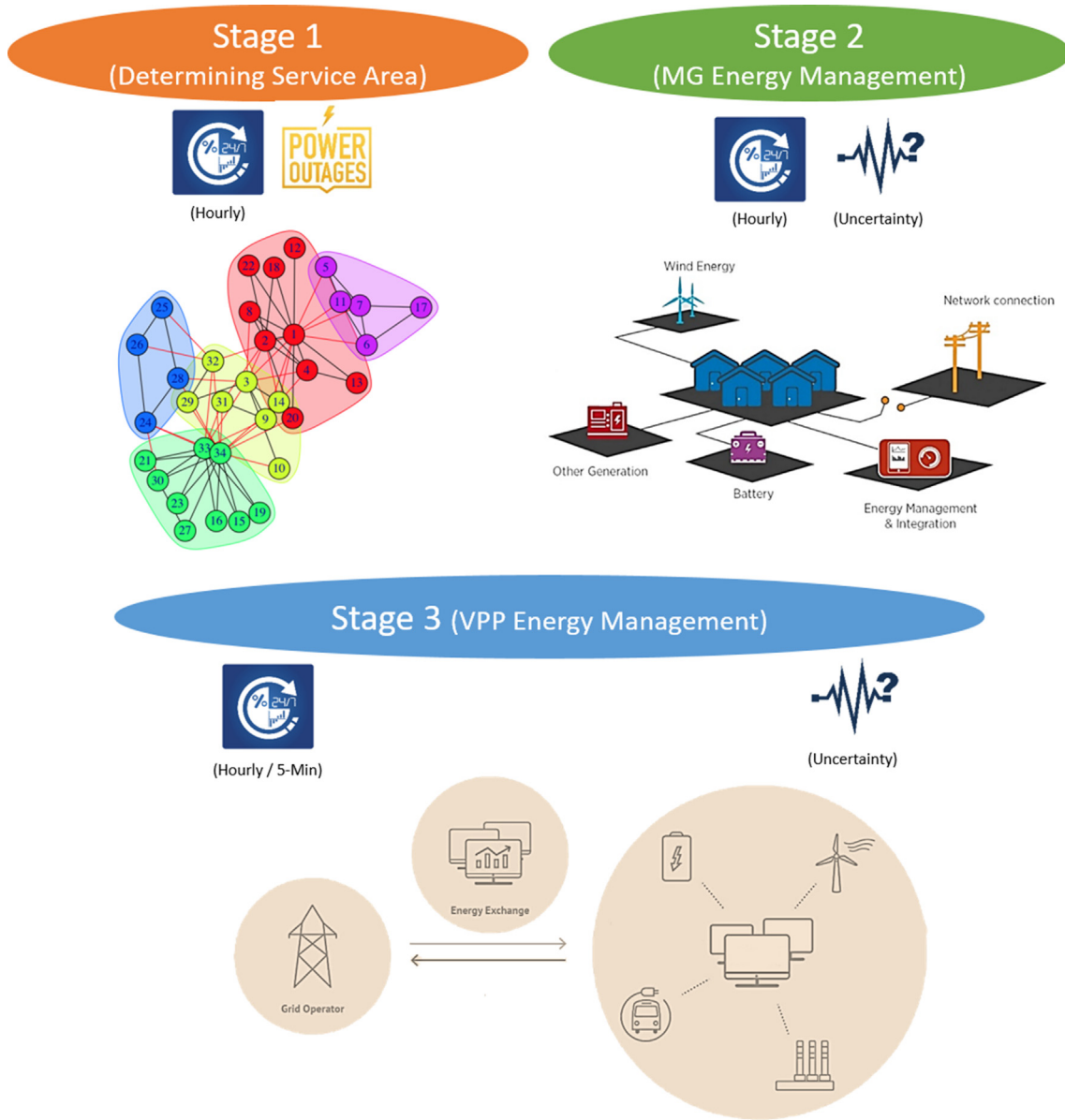


Fig. 1. The proposed model overview.

associated with the amount of energy stored, the maximum charging level, and the periodical discharging level have to be taken into account based on the storage system efficiency. These constraints are expressed using Eqs. (13)–(21).

$$c_t^{ES} = \gamma^{ES} P_t^{ES,Dis} \Delta t + \gamma^{ES} P_t^{ES,Ch} \Delta t \quad (13)$$

$$\gamma^{ES} = \frac{IC^{ES}}{E_R^{ES} \times LCN} \quad (14)$$

$$E_{t+1}^{ES} = E_t^{ES} - P_t^{ES,Dis} \Delta t / \eta^{ES,Dis} + P_t^{ES,Ch} \Delta t \cdot \eta^{ES,Ch} \quad (15)$$

$$SOC_t = E_t^{ES} / E_R^{ES} \quad (16)$$

$$SOC \leq SOC_t \leq \bar{SOC} \quad (17)$$

$$0 \leq P_t^{ES,Dis} \leq \chi_t^{ES,Dis} \cdot \bar{P}_t^{ES,Dis} \quad (18)$$

$$0 \leq P_t^{ES,Ch} \leq \chi_t^{ES,Ch} \cdot \bar{P}_t^{ES,Ch} \quad (19)$$

$$\chi_t^{ES,Dis} + \chi_t^{ES,Ch} \leq 1 \quad (20)$$

$$E_t^{ES} |_{t=1} = E_{INT}^{ES} \quad (21)$$

- **Controllable load:** DRPs are considered in MGs for adjusting the peak load demand. The controllable load cost is assumed to be a function of controllable load amount and it can be represented by a linear model given in (22)–(24).

$$P_{i,t}^L = P_{i,t}^{L0} - P_{i,t}^{CL} \quad (22)$$

$$C_{i,t}^{CL} = a^{CL} + b^{CL} P_{i,t}^{CL} \quad (23)$$

$$\zeta P_i^L \leq P_{i,t}^{CL} \leq \bar{\zeta} P_i^L \quad (24)$$

- **Power balance:** Considering the equipment existing within the service area of each MG, the power balance equation for the independent and coordinated MGs is stated as follows.

$$P_{i,t}^{CG} + P_{i,t}^{ES,Dis} + P_{i,t}^{Res} = P_{i,t}^L + P_{i,t}^{ES,Dis} + P_{i,t}^M \quad (25)$$

- **Energy exchange:** Having taken into consideration the energy

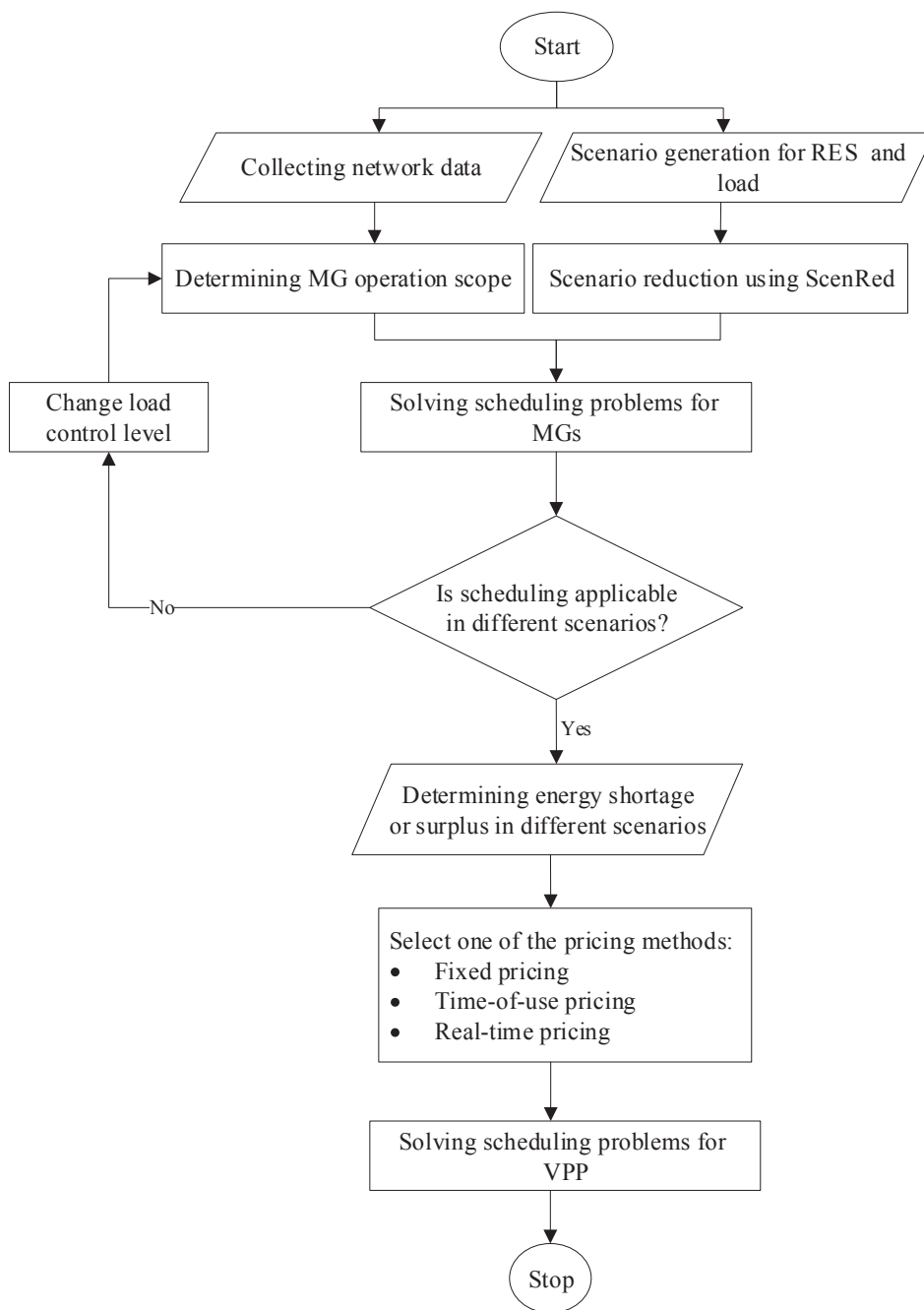


Fig. 2. Flowchart of the proposed model.

Table 1  
The case studies in the IEEE 118-bus network.

Case no.	MG operation mode	Scheduling method	Scheduling step
Case 1	Uncoordinated	Deterministic	1 h
Case 2	Coordinated	Deterministic	1 h
Case 3	Uncoordinated	Stochastic	1 h
Case 4	Coordinated	Stochastic	1 h
Case 5	Coordinated	Stochastic	5 min

$$P_{i,t}^M = P_{i,t}^{M,sell} - P_{i,t}^{M,buy} \tag{27}$$

$$0 \leq P_{i,t}^{M,sell} \leq P_i^M \times u_{i,t}^{sell} \tag{28}$$

$$0 \leq P_{i,t}^{M,buy} \leq P_i^M \times u_{i,t}^{buy} \tag{29}$$

$$u_{i,t}^{sell} + u_{i,t}^{buy} \leq 1 \tag{30}$$

$$C_{i,t}^M = \rho_t \times P_{i,t}^M \tag{31}$$

surplus or shortage at each hour in the service area of every MG, Eqs. (26)–(31) indicate how the energy is transacted with the distribution network.

$$\underline{P}_i^M \leq P_{i,t}^M \leq \bar{P}_i^M \tag{26}$$

### 3.3. VPP scheduling

In the third stage, the internal structure of other MGs is overlooked and it is modeled as a PCC. Therefore, depending upon the amount of power purchased or sold in each MG under different scenarios,



**Table 2**  
The required data of DGs, WTs and ESSs.

Distributed generation					ESS	Bus no.	Wind	
Unit	Bus.no	Cap. (kW)	Q <sup>max</sup> (kVAr)	Q <sup>min</sup> (kVAr)			Turbine	Bus no.
DG1	17	800	600	-600	ESS1	12	WT1	14
DG2	24	1000	800	-800	ESS2	26	WT2	27
DG3	51	900	800	-800	ESS3	40	WT3	42
DG4	59	1200	1000	-1000	ESS4	53	WT4	53
DG5	67	1000	800	-800	ESS5	72	WT5	74
DG6	76	1100	800	-800	ESS6	80	WT6	84
DG7	107	1500	1200	-1200	ESS7	90	WT7	88
DG8	7	200	150	-150	ESS8	110	WT8	96
DG9	33	300	200	-200			WT9	99
DG10	43	300	200	-200			WT10	112
DG11	88	200	100	-100				
DG12	103	500	300	-300				
DG13	113	300	150	-150				
DG14	117	300	150	-150				

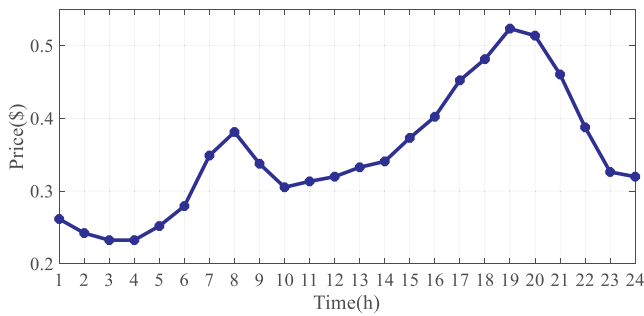


Fig. 3. Day-ahead forecasted electricity prices.

scheduling is carried out for other assets within the VPP service area. Each MG's goal to minimize its local costs is preserved and the VPP performs scheduling individually to maximize its profit. The objective function used in this stage is expressed via equation (32).

$$\max: F3 \left( \sum_k \text{profit}_{VPPk} \right) = \text{Max} \left[ \sum_k \left( \text{Income}_{VPPk} - \text{Cos } t_{VPPk} \right) \right] \quad (32)$$

$$\text{Income}_{VPPk} = \text{Income}_{VPPk}^{DG} + \text{Income}_{VPPk}^{sell} \quad (33)$$

$$\text{Cos } t_{VPPk} = \text{Cos } t_{VPPk}^{DG} + \text{Cos } t_{VPPk}^{buy} + \text{Cos } t_{VPPk}^{LC} \quad (34)$$

The maximization of the objective function (32) is subjected to the following limitations.

- **Load control:** For the loads with a high consumption peak, control options at five levels are considered. The modeling process is expressed through Eqs. (35)–(38).

$$P_{i,k,t}^{L,s} = \alpha_{i,k} \times PLoad_{i,t} - P_{i,k,t}^{LC,s} \quad (35)$$

$$P_{i,k,t}^{LC,s} \leq \alpha_{i,k} \times P_{i,t}^{LC,Max} \quad (36)$$

$$\sum_{k \in K} P_{i,k,t}^{LC,s} = \sum_{d=1}^D \sigma_{i,d,t}^{L,s} \times P_{i,d,t}^b \quad (37)$$

$$\sum_{d=1}^D \sigma_{i,d,t}^{L,s} \leq 1 \quad (38)$$

- **Generation units:** With regard to the generating units in each MG, the operating limitations of units have to be taken into account. Eqs. (39)–(41) express these limitations.

$$P_{m,k,t}^{DG,s} \leq \alpha_{r,k} \times P_m^{DG,Max} \quad (39)$$

$$P_{m,k,t}^{DG,s} \geq \alpha_{r,k} \times P_m^{DG,Min} \quad (40)$$

$$P_{n,k,t}^{W,s} \leq \alpha_{i,k} \times P_{n,t}^{W,Max} \quad (41)$$

- **Storage systems:** The storage system was modeled in stage three based on the resources in every MG. Eqs. (42)–(44) show the general limitations of the storage resources.

$$\gamma_{e,k,t}^{ES,s} \leq \alpha_{i,k}$$

$$PES_{e,k,t}^{ch,s} \leq \gamma_{e,k,t}^{ES,s} \times Rate_e^{ch,Max}$$

$$PES_{e,k,t}^{dis,s} \leq (1 - \gamma_{e,k,t}^{ES,s}) \times Rate_e^{dis,Max}$$

$$PES_{e,k,t}^{dis,s} \leq \alpha_{i,k} \times Rate_e^{dis,Max} \quad (42)$$

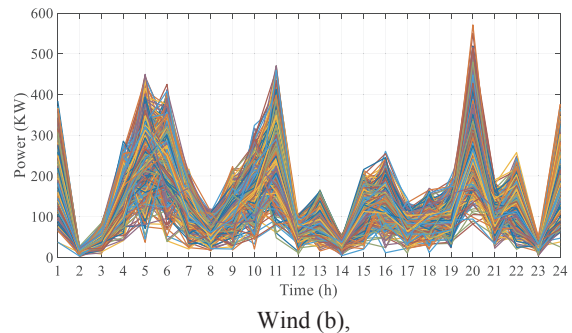
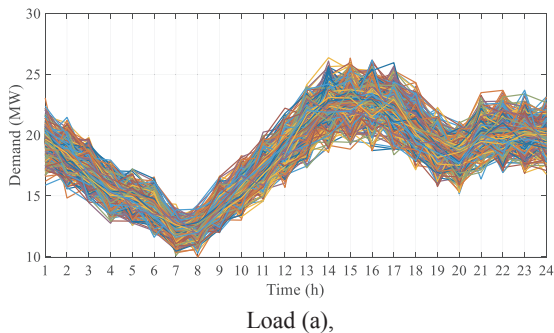


Fig. 4. Generated scenarios using Monte-Carlo.

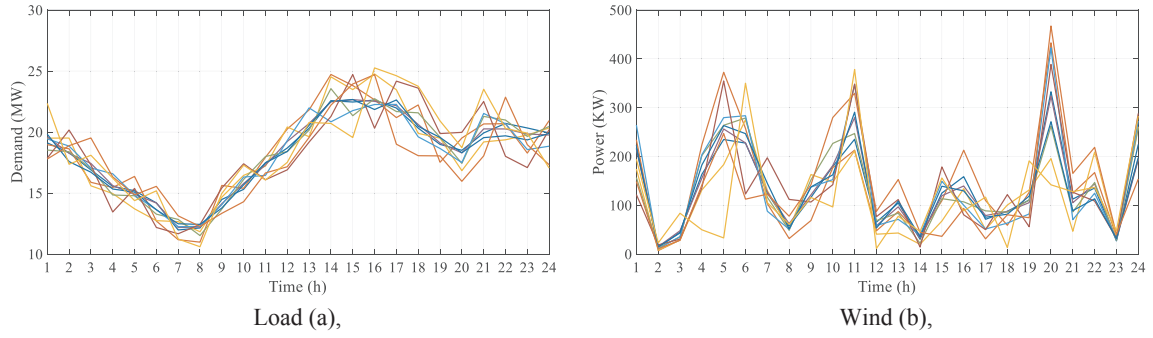


Fig. 5. Reduced scenarios using SCENRED.

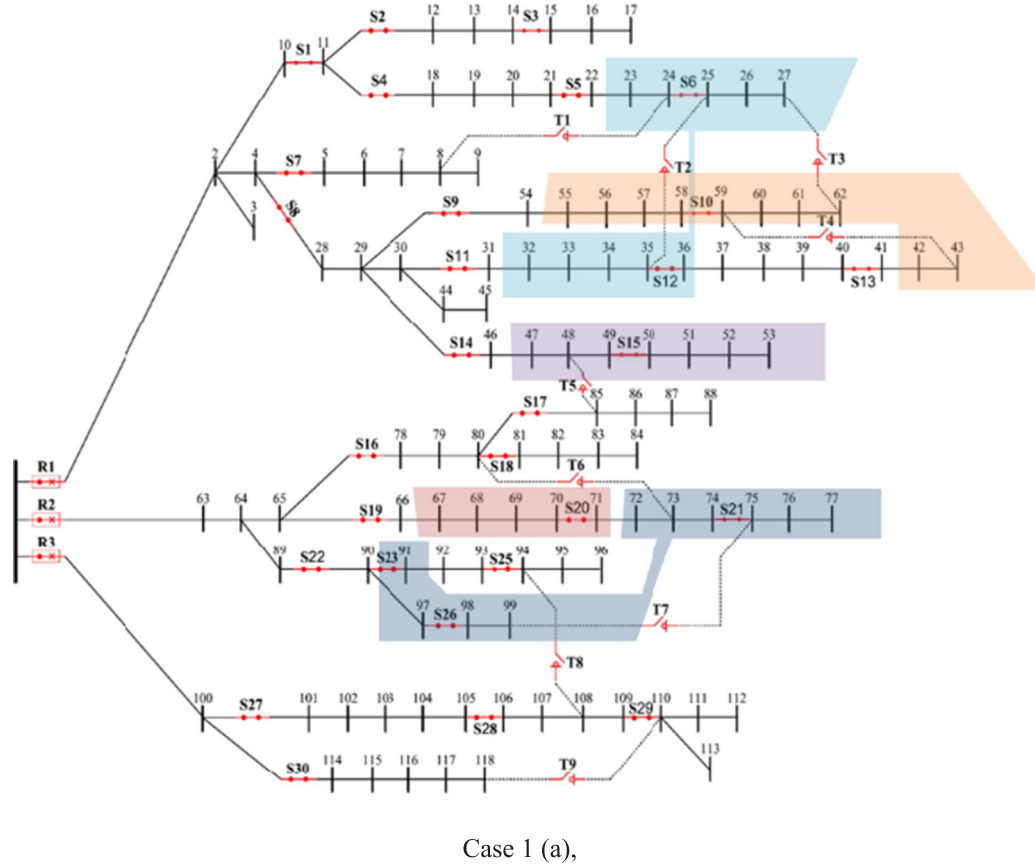


Fig. 6. Service areas of the MGs under deterministic scheduling conditions.

$$\begin{aligned}
 SOC_{e,k,t}^{ES,s} &\leq \alpha_{i,k} \times SOC_e^{ES,Max} \\
 SOC_{e,k,t}^{ES,s} &\geq \alpha_{i,k} \times SOC_e^{ES,Min} \\
 SOC_{e,k,t}^{ES,s} |_{t=0} &= SOC_e^{ES,initial}
 \end{aligned} \tag{43}$$

$$SOC_{e,k,t+1}^{ES,s} = SOC_{e,k,t}^{ES,s} + PES_{e,k,t}^{ch,s} \times \frac{\eta_e^{ES}}{Cap_e^{ES}} - PES_{e,k,t}^{dis,s} \times \frac{1}{\eta_e^{ES} \times Cap_e^{ES}} \tag{44}$$

• **Power balance in each MG:** Equation (45) is used to ensure the power balance at all network nodes.

$$\sum_{m=1}^{NDG} P_{m,k,t}^{DG,s} + \sum_{n=1}^{NWtr} P_{n,k,t}^{W,s} + \sum_{n=1}^{NPV} P_{n,k,t}^{PV,s} + \sum_{e=1}^{NES} PES_{e,k,t}^{dis,s} + P_{k,t}^M - \sum_{e=1}^{NES} PES_{e,k,t}^{ch,s} - \sum_{i=1}^{Nload} P_{i,k,t}^{L,s} = \sum_l flow_{l,t,\omega}^P \tag{45}$$

• **Network security constraints:** Given the importance of taking into account the security constraints on the distribution system, including the limitation on the power transmitted through the lines and the allowable variations of the voltage magnitude and angle, Eqs. (46)–(49) indicate how these constraints are applied.

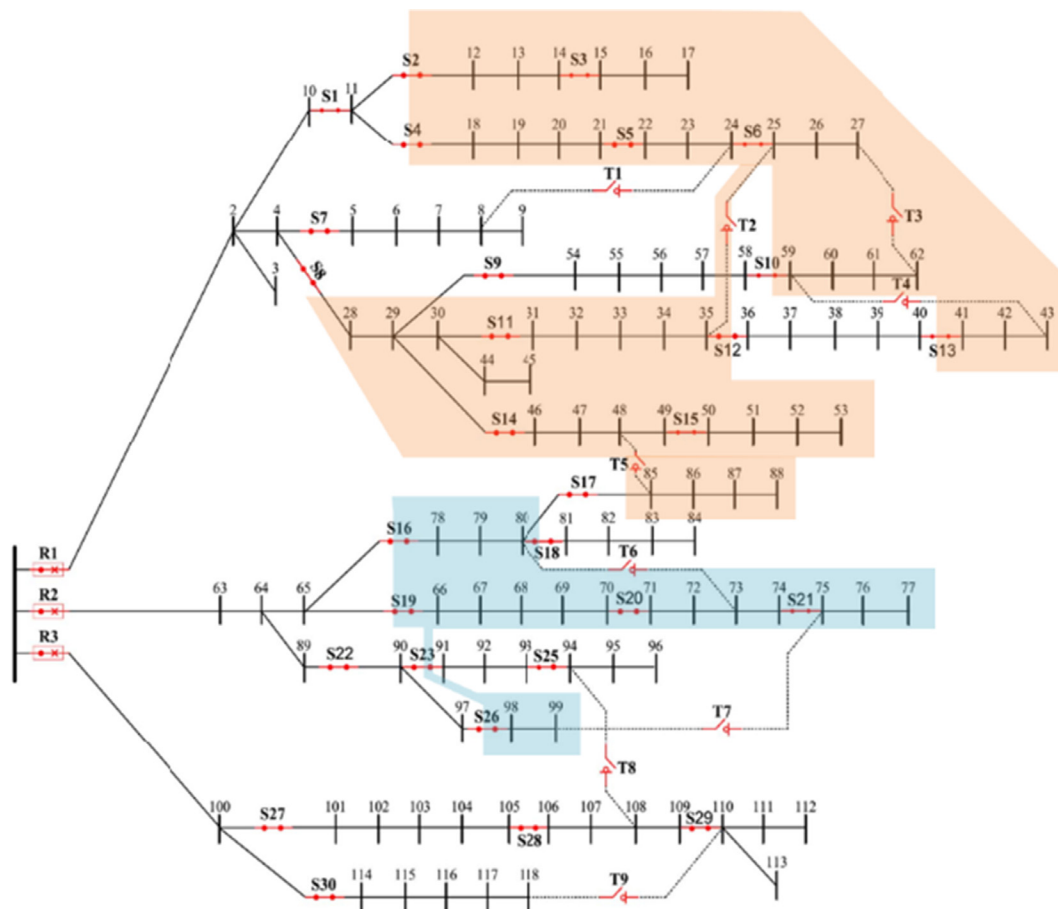
$$-\beta_l \times flow_{l,t,\omega}^{P,Max} \leq flow_{l,t,\omega}^P \leq \beta_l \times flow_{l,t,\omega}^{P,Max} \tag{46}$$

$$-\beta_l \times flow_{l,t,\omega}^{Q,Max} \leq flow_{l,t,\omega}^Q \leq \beta_l \times flow_{l,t,\omega}^{Q,Max} \tag{47}$$

$$\alpha_{i,k} \times 0.9 \leq V_{i,k,t,\omega} \leq \alpha_{i,k} \times 1.1 \tag{48}$$

$$-\alpha_{i,k} \times \delta^{Max} \leq \delta_{i,k,t,\omega} \leq \alpha_{i,k} \times \delta^{Max} \tag{49}$$

• **Power flow:** In this stage, an effective linear approximation is used to calculate the voltage angle and magnitude at the network buses [32]. The equations for calculating the active and reactive power and the conditions for removing the power flow constraint when the

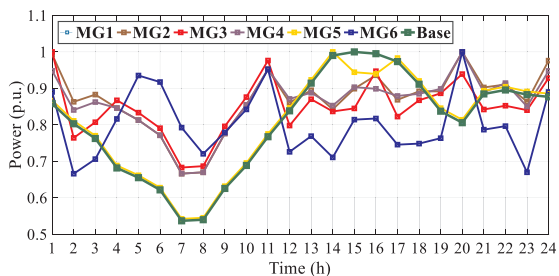


Case 2 (b),

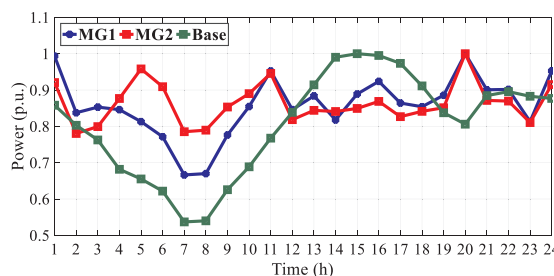
Fig. 6. (continued)

**Table 3**  
Detailed service areas of the MGs\_Case 1 and Case 2.

	Number of MGs	Number of points covered	ESS (kW)	Wind energy capacity (kW)	Generation capacity (kW)	Load supplied (kW)	Resiliency
Case 1	6	7	500	500	800	454.51	30.29%
		11	500	500	1300	1442.37	
		8	500	500	900	1017.79	
		12	0	0	1500	1615.94	
		5	0	0	1000	941.27	
Case 2	2	11	1000	1000	1100	1406.78	33.98%
		46	1500	2500	4700	5372.44	
		17	1000	1000	2100	2344.31	



Case 1 (a),



Case 2 (b),

Fig. 7. The load curve for the MGs.



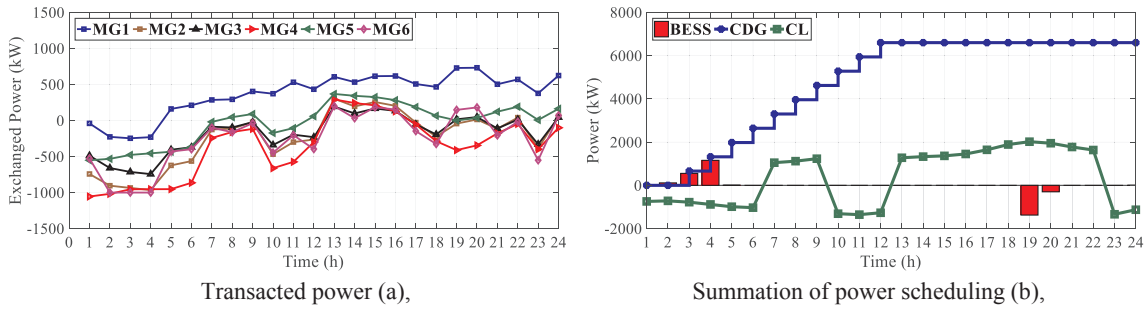


Fig. 8. The energy transaction curve in each MG and the method of scheduling in Case 1.

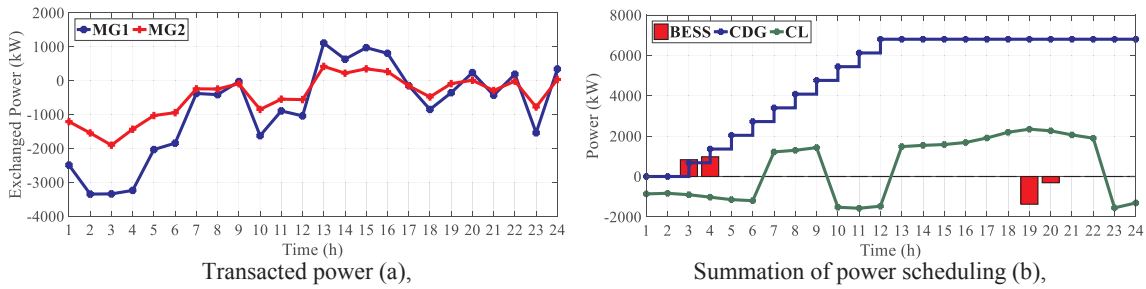


Fig. 9. The power transaction curve in each MG and the method of scheduling in Case 2.

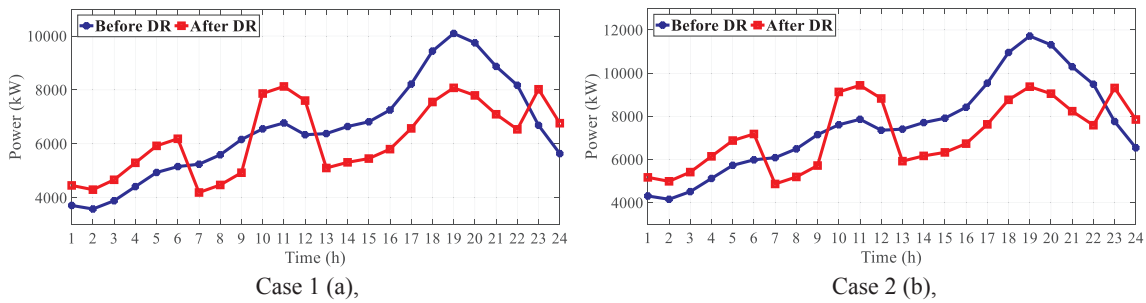


Fig. 10. The impact of the DRP on the consumption pattern.

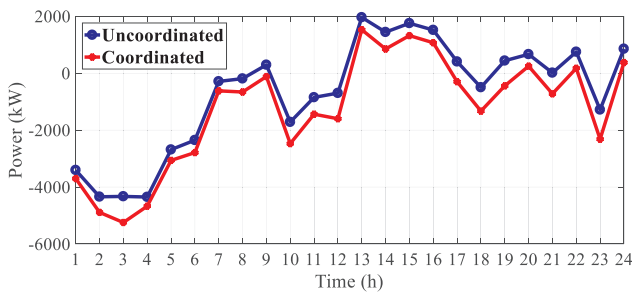


Fig. 11. The total amounts of energy purchased and sold in Case 1 and Case 2.

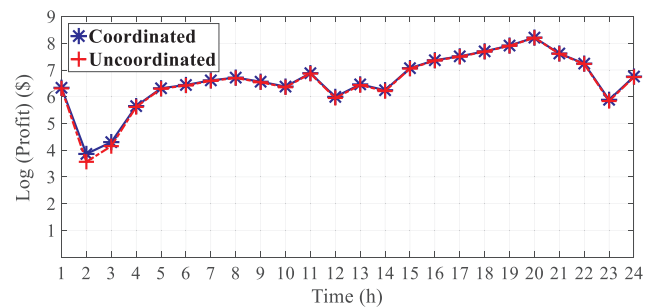


Fig. 12. The logarithmic diagram of the hourly profit of the VPP in Case 1 and Case 2.

Table 4  
The operation results of MGs in Case 1 and Case 2.

	Operation cost (\$)	Load supplied (MW)	Thermal units operation cost (\$)	ESS (\$)	DRP (\$)	Power exchange (\$)	Profit (\$)
Case1	40819.645	156.336	34656.520	140.147	2710.062	3310.916	19167.472
Case2	47282.025	181.467	35702.840	139.806	3139.749	8299.630	19554.161

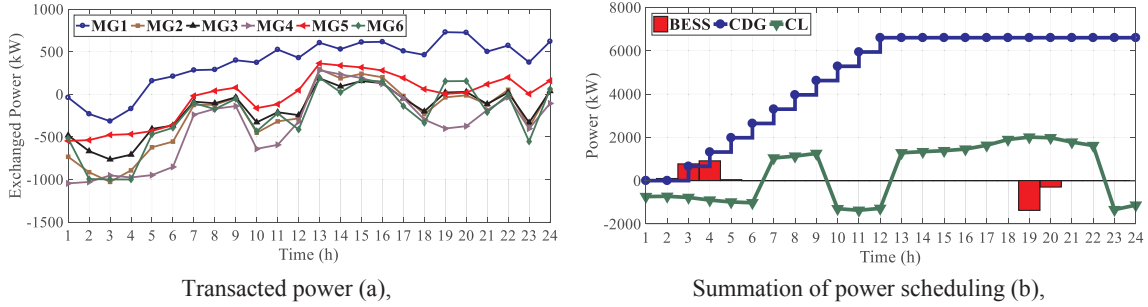


Fig. 13. The energy transaction and optimal schedule of each MG in Case 3.

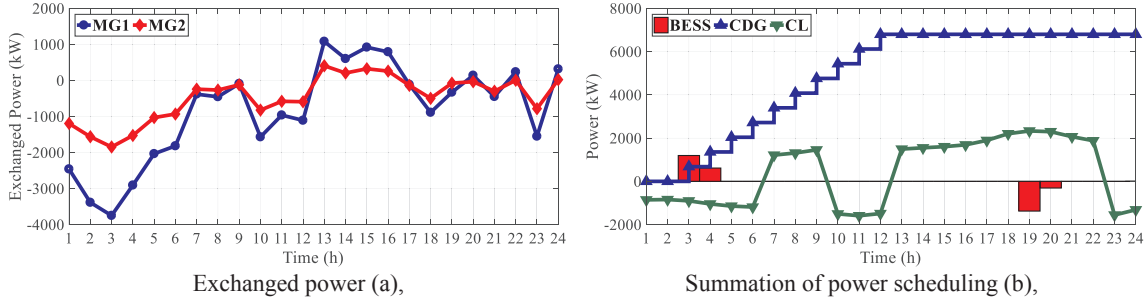


Fig. 14. The diagram of power transaction and scheduling in each MG in Case 4.

Table 5  
The operation results of the MGs in Case 3 and Case 4.

	Demand (MW)	Cost (\$)					Profit (\$)
		Operation	Thermal units (\$)	ESS (\$)	DRP (\$)	Power exchange (\$)	
Case3	156.336	41030.056	34658.520	140.147	2729.248	3502.141	18766.752
Case4	181.467	47528.760	35702.840	139.806	3162.019	8524.095	19188.114

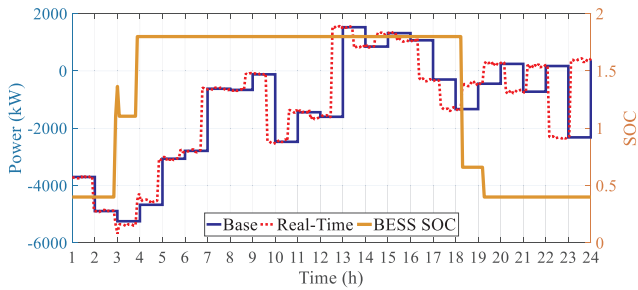


Fig. 15. 5-minute energy purchase and sale in Case 5.

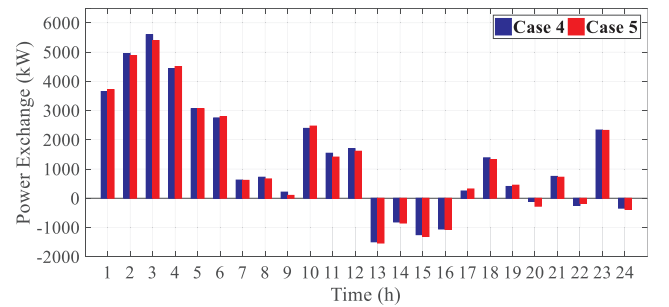


Fig. 16. Comparative illustration of power transactions in Case 4 and Case 5.

line is not operated are stated through Eqs. (50)–(54).

$$F1_l = \frac{\eta_l}{r_l^2 + x_l^2}, \quad F2_l = \frac{x_l}{r_l^2 + x_l^2} \quad (50)$$

$$\begin{aligned} flow_{l,t,\omega}^P &= Zflow_{l,t,\omega}^P + \sum_{\forall k \in K} [\delta_{i,k,t,\omega} - \delta_{j,k,t,\omega}] \times F2_l + \sum_{\forall k \in K} [V_{j,k,t,\omega} - V_{i,k,t,\omega}] \\ &\times F1_l \end{aligned} \quad (51)$$

$$\begin{aligned} flow_{l,t,\omega}^Q &= Zflow_{l,t,\omega}^Q + \sum_{\forall k \in K} [\delta_{i,k,t,\omega} - \delta_{j,k,t,\omega}] \times F1_l + \sum_{\forall k \in K} [V_{j,k,t,\omega} - V_{i,k,t,\omega}] \\ &\times F2_l \end{aligned} \quad (52)$$

$$-(1 - \beta_l) \times BigM \leq Zflow_{l,t,\omega}^P \leq (1 - \beta_l) \times BigM \quad (53)$$

$$-(1 - \beta_l) \times BigM \leq Zflow_{l,t,\omega}^Q \leq (1 - \beta_l) \times BigM \quad (54)$$

Table 6  
The operation results of the MGs in Case 5.

Operation cost (\$)	Load demand (kW)	Thermal units (\$)	EES (\$)	DRP (\$)	Power exchange (\$)	Profit (\$)
47261.103	181.467	35702.840	139.806	3138.343	8280.114	19553.604

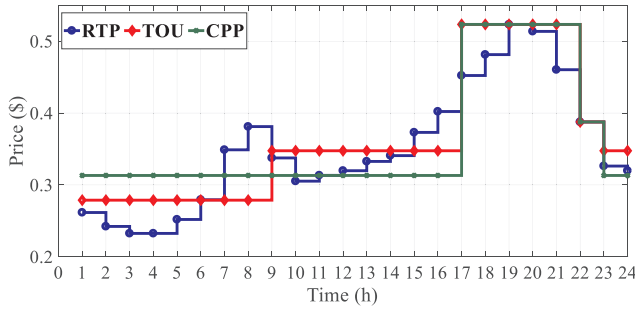


Fig. 17. The energy purchase and sale prices in different pricing mechanisms.

Table 7

The profit made in the third stage using different pricing mechanisms in Case 5.

	RTP	TOU	CPP
Deterministic scheduling (\$)	19554.161	21509.758	18864.357
Stochastic scheduling (\$)	19188.114	21009.506	18409.092
5-minute scheduling (\$)	19533.604	21483.580	18839.892

- **Constraints of EVs:** When modeling EVs, it is assumed that their trip, their arrival, and their departure times are determined. Hence, considering the distance driven by each vehicle, and the hours of their presence in the parking, the equations for the operation of the EVs are represented in (55–60).

$$E_{e,t}^{\text{stored}} = E_{e,t-1}^{\text{stored}} + (\eta_c^{\text{ch}} \times P_{e,t}^{\text{ch}} - \frac{P_{e,t}^{\text{dis}}}{\eta_e^{\text{dis}}}) \times \Delta t - E_{e,t}^{\text{trip}} \quad (55)$$

$$E_{e,t}^{\text{trip}} = P_{e,t}^{\text{trip}} \times \Delta t \quad (56)$$

$$P_{e,t}^{\text{ch}} \leq P_{e,t}^{\text{ch,limit}} \times x_{e,t}^{\text{ch}} \quad (57)$$

$$P_{e,t}^{\text{dis}} \leq P_{e,t}^{\text{dis,limit}} \times x_{e,t}^{\text{dis}} \quad (58)$$

$$0 \leq x_{e,t}^{\text{ch}} + x_{e,t}^{\text{dis}} \leq 1 \quad (59)$$

$$\sum_e x_{e,t}^{\text{ch}} + x_{e,t}^{\text{dis}} \leq EV^{\text{available}} \quad (60)$$

#### 4. Solution method

In this paper, a three-stage stochastic framework is proposed for the energy management of a VPP and its MGs. In the first stage, MGs scheduling is done to maximize the maximum possible load supply in the network. MGs that can be controlled with a coordinated approach are identified, considering the network configuration. The service area of each MG is defined, considering the switches on the main feeders and also the capacity of each feeder. The MG can partly restore controllable loads once an error occurs. In the second stage, the energy management is implemented for each MG and the uncertainty of RESs and loads is taken into account. The third stage investigates the optimal scheduling of the VPP with respect to the energy sale/purchase requirements of the MGs and also, the assets out of MGs. A VPP can be comprised of one or several MGs besides different types of loads and generation technologies. Scheduling is carried out with three pricing mechanisms, i.e. CPP, TOU, and RTP, within hourly and 5-minute periods. Also, DRPs and storage systems, known as EVs are used to control the unbalance costs and increase the VPP profit. The concept of the presented model is indicated in Fig. 2.

- Collecting detailed data of the studied distribution network, including the load pattern characteristics, renewable power generation, generating units, storage systems, network configuration, and

protective switches.

- Determining the operation of the MGs both in uncoordinated and coordinated modes in stage one with respect to the uncertainties of load demand and RESs.
- Generating the data required for the second stage, including the assets in each MG, load pattern, and the renewable power generation both in coordinated and uncoordinated modes.
- Coordinated and uncoordinated scheduling of MGs, considering the uncertainties due to the load demand and RESs.
- Scheduling the VPP, taking into consideration different pricing mechanisms and EVs.

#### 5. Simulation results

In this section, the performance of the proposed model for deterministic and stochastic analysis in distribution networks is investigated. Simulation has been done using a PC with Intel Core i5 CPU @3.2 GHz and 8 GB RAM. The proposed problem has been solved using GUROBI Solver in GAMS software ver. 27.2.

##### 5.1. Data

In this paper, an IEEE 118-Bus modified distribution network comprised of 3 feeders, 118 buses, 3 breakers, 30 sectionalizers, and 9 tie lines is used as the test network to study the proposed framework [32]. The total active and reactive power demands for this network are 22.71 MW and 17.04 MVar, respectively. The required data for the location and capacity of the distributed generation (DGs) units, WTs, and ESSs are represented in Table 2. In this network, 7 units (DG1 to DG7) of the 14 existing units can serve as master units. Therefore, the maximum number of MGs that can be formed is 7. The capacity, charging and discharging rates, output, and the state of charge (SoC) of the storage units are set to 500 kW, 100kWh, 85%, and 60%, respectively. The capacity of the WTs is also 500 kW. Fig. 3 depicts the day-ahead forecasted electricity prices over 24 h on a typical day.

A set of 1000 scenarios is generated for scheduling purposes as shown in Fig. 4. The scenarios have been generated using the Monte-Carlo simulation with Weibull and normal probability distribution functions for wind and load, respectively. With respect to the high computational burden, the number of scenarios has been reduced to 10 using SCENRED. The reduced scenarios are shown in Fig. 5. To create the required resilience, it is assumed that loads greater than 400 kW can change their consumption by 50% in a stepwise manner. The following five cases have been analyzed to verify the performance of the presented three-stage model. In all Cases, outage in two of the three main feeders of the network, namely “feeders (1–63) and (1–2)”, is taken into account to provide the faulty conditions in the studied network and determine the service areas of the MGs. In addition, a VPP is defined in the area of faulty feeders for energy management in the third stage. Table 1 represents the detail of each case.

##### 5.2. Case 1 and Case 2

After solving the first stage of the proposed method, the obtained service areas of the MGs in Case 1 and Case 2 are shown in Fig. 6a and b, respectively.

As can be observed in Fig. 6a and b, a higher load demand has been supplied in the coordinated operation case and the MGs are managed to cover more points in the main network by sharing power. In Case 1 and Case 2, six and two MGs are formed, respectively. In Case 1, the number of MGs is equal to the number of main generating units. The formation of two MGs in the second case implies that some MGs could not follow the coordinated operation and participate in the supply of each other's loads due to the locations of their main generating units. In other words, the power transaction between all MGs is not possible in the proposed method because the power transaction is impossible given the

network configuration, the free capacity of the common feeders, and the location of the MGs. The capacity of the equipment and the amount of load supplied in each MG in Cases 1 and 2 are listed in Table 3 to identify the quantity of the equipments within the optimal service areas of the MGs.

As a result of different assets, the operation pattern of MGs, including their load curve, the WTs' power output, and the storage system capacities, would be different. Besides, the operation conditions of each MG are assessed, considering its specifications and location. Fig. 7a and b illustrate the load curves of the MGs in Case 1 and Case 2, respectively.

As seen in Fig. 7, only MGs 1 and 5 have followed the main load curve in Case 1 due to the small amount of load in the areas covered by these MGs and also, the impossibility of using load control in these MGs. This is because loads more than 400 kW are allowed to use the load control option. The sale of additional generation and compensation of the generation deficit in Case 1 is depicted in Fig. 8a. As seen in Fig. 8a, all MGs sold their energy at peak-price hours. MG 1 was always willing to sell its energy after the initial hours due to the shortage of the covered load and the low cost of energy generation. The reason for the purchase of energy in the beginning hours was the low energy prices and the ramping limitations. The overall diagram of the total MGs operation is illustrated in Fig. 8b to identify the frequency of using the DRP and storage devices.

Based on Fig. 8b, MGs try to control the energy supply cost at peak hours though purchasing and storing energy during the early hours. The generation surplus and deficit in Case 2 are presented in Fig. 9. As seen in Fig. 9a, the surplus power generated is sold only during peak hours, which could be attributed to the coverage of more points in the coordinated operation case and the use of additional energy for the supply of load at these points. In other words, the adjacent MGs can compensate for the deficit in the power generation of an MG.

The optimal hourly scheduling of the assets has been depicted in Fig. 9b. Similarly to Fig. 8b, the power generation shows a stepwise trend until it reached the maximum capacity. The reason for the stepwise generation curve is the ramping rate limitations of the generating units. In addition, the ESS mitigates the operating cost during these hours by shifting a fraction of the generation to the consumption peak.

The load consumption pattern in the absence or presence of the DRP is presented in Fig. 10a and b in Case 1 and Case 2, respectively. As seen in Fig. 10a, the use of the DRP capable of load shifting or curtailment, reduces the load peak. As a result, the load peak decreases by 19.5% and the number of peaks rises to three peaks. The reason for the emergence of a peak at hours 6:00 and 11:00 is the low price of energy during these hours. In the second case shown in Fig. 10b, the consumption after using the DRP follows the same pattern.

In Fig. 11, the amount of energy purchased and sold at different hours is indicated. As it is shown in Fig. 11, MGs in the coordinated operation mode sell more and purchase less power from the network. Table 4 represents the operation details of the second stage in Case 1 and Case 2.

The VPP performs scheduling for the total load within its service area. The hourly profit values in Case 1 and Case 2 are shown in Fig. 12. As seen in Fig. 12, the coordinated scheduling of the MGs increases the VPP profit. The values of total profit in Case 1 and Case 2 are \$19167.472 and \$19554.161, respectively. The increase in profit in the second case is due to the better performance of the VPP in the energy transaction over the beginning hours of the scheduling period.

### 5.3. Case 3 and Case 4

The energy transaction with the distribution network and the optimal schedule in Case 3 and Case 4 are depicted in Figs. 13 and 14. A comparison of Figs. 13 and 14 with the purchase and sale values in the deterministic cases, shown in Figs. 8 and 9, reveals that the amount of power transacted has increased due to the fluctuations in the load

demand and wind power generation.

Table 5 represents the operating costs of Case 3 and Case 4, showing an increase in the costs compared to the first two cases.

### 5.4. Case 5

In this case, the coordinated scheduling in real conditions is studied. A 5-minute time resolution is considered and the feasibility of scheduling and the coverage of real-time fluctuations are analyzed. The total hourly energy sale of the MGs in Case 5 is shown in Fig. 15.

Based on Fig. 15, the 5-minute scheduling follows the deterministic scheduling pattern with the aid of EVs and DRPs, covering the existing fluctuations. The operation results in this case are indicated in Table 6.

Table 6 shows that the operating cost of Case 5 has reduced compared to that of Case 4, mainly due to the energy purchase from the network. Fig. 16 depicts the comparative representation of power transactions in Case 4 and Case 5. This figure indicates that Case 5 is associated with a lower cost due to the energy purchase and a higher profit due to energy sale over the majority of intervals in comparison with Case 4.

The profit gained using the three mechanisms, i.e. RTP, TOU, and CPP, is shown in Table 6 to study the impact of the method used for calculating the VPP profit in different markets. In addition, the three pricing mechanisms are depicted in Fig. 17.

According to Table 7, the profit made through TOU pricing in the three simulation models is higher. As for the CPP, since the price is lower during the off-peak hours, the VPP profit decreases. Besides, the RTP profit is average and more realistic.

## 6. Conclusion

This paper proposed a three-stage stochastic model for the simultaneous scheduling of a virtual power plant (VPP) and microgrids (MGs), taking into consideration the uncertainties due to renewable power generation and load demand. The problem was presented aimed at maximizing the VPP profit with respect to the optimal scheduling of MGs, which was defined as total operating cost minimization, taking into account different pricing mechanisms. The scenarios of wind power generation and load demand were generated using the Monte-Carlo simulation and SCENRED was used to reduce the number of scenarios to balance the computational burden of the problem. The presented model considered the network configuration and power flow equations to avoid any unreal power transaction. Afterward, the model was simulated for five different cases, addressing the coordinated and uncoordinated operation modes. The results obtained showed that the coordinated operation of MGs would lead to mitigating the load supply cost, and considering the uncertainties resulted in increasing the operating cost. It was also verified that the TOU mechanism would provide the VPP with a higher profit compared to other pricing mechanisms.

### Declaration of Competing Interest

The authors declare that they have no known competing financial interests or personal relationships that could have appeared to influence the work reported in this paper.

### References

- [1] Nosratabadi SM, Hooshmand R-A, Gholipour E, Parastegari M. A new simultaneous placement of distributed generation and DR resources to determine virtual power plant. *Int Trans Electr Energy Syst* 2016;26(5):1103–20.
- [2] Zhang C, Xu Y, Dong ZY, Ma J. Robust Operation of MGs via two-stage coordinated energy storage and direct load control. *IEEE Trans Power Syst* 2017;32(4):2858–68.
- [3] Bao Z, Zhou Q, Yang Z, Yang Q, Xu L, Wu T. A multi time-scale and multi energy-type coordinated MG scheduling solution—part I: model and methodology. *IEEE Trans Power Syst* 2015;30(5):2257–66.

- [4] Olivares DE, Cañizares CA, Kazerani M. A centralized energy management system for isolated MGs. *IEEE Trans Smart Grid* 2014;5(4):1864–75.
- [5] Wang Z, Chen B, Wang J, Kim J. Decentralized energy management system for networked MGs in grid-connected and islanded modes. *IEEE Trans Smart Grid* 2016;7(2): p. 1097–1105.
- [6] Wang Y, Mao S, Nelms RM. On hierarchical power scheduling for the macrogrid and cooperative MGs. *IEEE Trans Ind Inf* 2015;11(6):1574–84.
- [7] Hussain A, Bui V, Kim H. A resilient and privacy-preserving energy management strategy for networked MGs. *IEEE Trans Smart Grid* 2018;9(3):2127–39.
- [8] Aziz T, Masood N-A, Deeba SR, Tushar W, Yuen C. A methodology to prevent cascading contingencies using BESS in a renewable integrated MG. *Int J Electr Power Energy Syst* 2019;110:737–46.
- [9] Tabar VS, Ghassemzadeh S, Tohidi S. Energy management in hybrid MG with considering multiple power market and real time DR. *Energy* 2019;174:10–23.
- [10] Ju C, Wang P, Goel L, Xu Y. A two-layer energy management system for MGs with hybrid energy storage considering degradation costs. *IEEE Trans Smart Grid* 2018;9(6):6047–57.
- [11] Andishgar MH, Gholipour M, Hooshmand R-A. Improved secondary control for optimal unbalance compensation in islanded MGs with parallel DGs. *Int J Electr Power Energy Syst* 2020;116:105535.
- [12] Rezaei N, Ahmadi A, Khazali AH, Guerrero JM. Energy and frequency hierarchical management system using information gap decision theory for islanded MGs. *IEEE Trans Ind Electron* 2018;65(10):7921–32.
- [13] Thirugnanam K, Kerk SK, Yuen C, Liu N, Zhang M. Energy management for renewable MG in reducing diesel generators usage with multiple types of battery. *IEEE Trans Ind Electron* 2018;65(8):6772–86.
- [14] Farzan F, Jafari MA, Masiello R, Lu Y. Toward optimal day-ahead scheduling and operation control of MGs under uncertainty. *IEEE Trans Smart Grid* 2015;6(2):499–507.
- [15] Wang Z, Chen B, Wang J, Begovic MM, Chen C. Coordinated energy management of networked MGs in distribution systems. *IEEE Trans Smart Grid* 2015;6(1):45–53.
- [16] Li Z, Shahidehpour M, Aminifar F, Alabdulwahab A, Al-Turki Y. Networked MGs for enhancing the power system resilience. *Proc IEEE* 2017;105(7):1289–310.
- [17] Khavari F, Badri A, Zangeneh A. Energy management in multi-MGs considering point of common coupling constraint. *Int J Electr Power Energy Syst* 2020;115:105465.
- [18] Nikmehr N, Najafi-Ravadanegh S, Khodaei A. Probabilistic optimal scheduling of networked MGs considering time-based DR programs under uncertainty. *Appl Energy* 2017;198:267–79.
- [19] Wang D, Qiu J, Reedman L, Meng K, Lai LL. Two-stage energy management for networked MGs with high renewable penetration. *Appl Energy* 2018;226:39–48.
- [20] Shafiekhani M, Badri A, Shafie-khah M, Catalão João PS. Strategic bidding of virtual power plant in energy markets: a bi-level multi-objective approach. *Int J Electr Power Energy Syst* 2019;113:208–19.
- [21] Wei C, Xu J, Liao S, Sun Y, Jiang Y, Ke D, et al. A bi-level scheduling model for virtual power plants with aggregated thermostatically controlled loads and renewable energy. *Appl Energy* 2018;224:659–70.
- [22] Abdolrasol MGM, Hannan MA, Mohamed A, Amiruldin UAU, Abidin IBZ, Uddin MN. An optimal scheduling controller for virtual power plant and MG integration using the binary backtracking search algorithm. *IEEE Trans Ind Appl* 2018;54(3):2834–44.
- [23] Zhang Gao, Jiang Chuanwen, Wang Xu, Li Bosong, Zhu Huangang. Bidding strategy analysis of virtual power plant considering DR and uncertainty of renewable energy 11: Institution of Engineering and Technology; 2017.
- [24] Al-Awami AT, Amlah NA, Muqbel AM. Optimal DR bidding and pricing mechanism with fuzzy optimization: application for a virtual power plant. *IEEE Trans Ind Appl* 2017;53(5):5051–61.
- [25] Toubeau J, De Grève Z, Vallée F. Medium-term multimarket optimization for virtual power plants: a stochastic-based decision environment. *IEEE Trans Power Syst* 2018;33(2):1399–410.
- [26] Wang J, Shen X, Guo Q, Xiong W, editors. Economic analysis of multi-energy virtual power plant considering market information. In: 2017 IEEE conference on energy internet and energy system integration (EI2); 2017.
- [27] Hadayeghparast S, SoltaniNejad Farsangi A, Shayanfar H. Day-ahead stochastic multi-objective economic/emission operational scheduling of a large scale virtual power plant. *Energy* 2019;172:630–46.
- [28] Ju L, Tan Q, Lu Y, Tan Z, Zhang Y, Tan Q. A CVaR-robust-based multi-objective optimization model and three-stage solution algorithm for a virtual power plant considering uncertainties and carbon emission allowances. *Int J Electr Power Energy Syst* 2019;107:628–43.
- [29] Liu Y, Li M, Lian H, Tang X, Liu C, Jiang C. Optimal dispatch of virtual power plant using interval and deterministic combined optimization. *Int J Electr Power Energy Syst* 2018;102:235–44.
- [30] Yu S, Fang F, Liu Y, Liu J. Uncertainties of virtual power plant: problems and countermeasures. *Appl Energy* 2019;239:454–70.
- [31] Nosratabadi SM, Hooshmand R-A, Gholipour E. A comprehensive review on microgrid and virtual power plant concepts employed for distributed energy resources scheduling in power systems. *Renew Sustain Energy Rev* 2017;67:341–63.
- [32] Hooshmand R-A, Nosratabadi SM, Gholipour E. Event-based scheduling of industrial technical virtual power plant considering wind and market prices stochastic behaviors - a case study in Iran. *J Clean Prod* 2018;172:1748–64.
- [33] Mousavizadeh S, Haghifam M-R, Shariatkah M-H. A linear two-stage method for resiliency analysis in distribution systems considering renewable energy and DR resources. *Appl Energy* 2018;211:443–60.